

# Vascular endothelial cells in cultures on nanocomposite silver/hydrocarbon plasma polymer films with antimicrobial activity

L. BACAKOVA<sup>\*</sup>, H. KOSHELYEV<sup>a</sup>, L. NOSKOVA, A. CHOUKOUROV<sup>a</sup>, O. BENADA<sup>b</sup>, A. MACKOVA<sup>c</sup>, V. LISA,  
H. BIEDERMAN<sup>a</sup>

<sup>a</sup>Institute of Physiology, Academy of Sciences of the Czech Republic, Videnska 1083, 142 20 Prague 4, Czech Republic

<sup>a</sup>Department of Macromolecular Physics, Faculty of Mathematics and Physics, Charles University,  
V Holešovickach 2, 182 00 Prague 8, Czech Republic

<sup>b</sup>Institute of Microbiology, Academy of Sciences of the Czech Republic, Videnska 1083, 142 20 Prague 4, Czech Republic

<sup>c</sup>Nuclear Physics Institute, Academy of Sciences of Czech Republic, 250 68 Rez near Prague, Czech Republic

Bioactive hydrocarbon plasma polymer films containing 3, 30 and 39 at.% of Ag in the form of nanoclusters were deposited on microscopic glass slides using an unbalanced magnetron with an Ag target operated in the dc mode in a working gas mixture of n-hexane and argon. The films were seeded with bovine pulmonary artery endothelial cells (line CPAE) or inoculated with bacterium *Escherichia coli*. The CPAE cells on films with 3 at.% Ag adhered and grew to a similar extent as on the control pure hydrocarbon films or glass slides. By contrast, the CPAE cell adhesion on films with 30 or 39 at.% of Ag was very low, and the cells died before day 7 of cultivation. In bacterial cultures, all silver-containing films attenuated the growth of *E. coli* as opposed to pure hydrocarbon plasma polymer films.

(Received March 1, 2008; accepted June 30, 2008)

**Keywords:** Hard hydrocarbon coating, Nanostructure, Endothelium, Focal adhesion plaques, von Willebrand factor, *E. coli*

## 1. Introduction

Hard hydrocarbon plasma polymers, deposited as organic films using plasma polymerization of gaseous hydrocarbon precursors and additional positive ion bombardment, have been proposed for various industrial applications, such as for microelectronics and for protective and optical coatings [1, 2]. In addition, these materials can be advantageously used in biomedicine and other biotechnologies. For example, hard hydrocarbon plasma polymers and related materials, such as amorphous hydrogenated diamond-like carbon, have been used for coating bone and joint prostheses, artificial heart valves, vascular stents, blood pumps and other blood-contacting devices in order to increase their wear resistance, smoothness, hydrophobicity and blood compatibility [3-6]. The advantageous physical and chemical properties of these films, as well as their low attractiveness for adhesion of thrombocytes, inflammatory cells and microorganisms, could be further modified by adding metallic ions. Among these ions, great attention has been paid to silver, due to its remarkable antimicrobial activity. Silver has been used as an important component of bioactive wound dressings [7], eye drops, urinary and vascular catheters [8, 9], artificial vascular grafts and heart valves [10, 11], devices for bone fixation [12], orthopaedic and dental grafts [13], bone cements [14], three-dimensional scaffolds designed for engineering various tissues, e.g. bone [15, 16], and sponges for potential construction of bioartificial skin [17].

The incorporation of silver into a hydrocarbon plasma polymer matrix has been attempted in several studies (for a review, see [2]); however, knowledge about the behaviour of these composite materials in biological systems, especially their influence on eukaryotic anchorage-dependent cells, is still limited. This study therefore investigated the adhesion, growth and maturation of vascular endothelial cells in cultures on Ag/hydrocarbon plasma polymer films, and made a correlation with the physicochemical properties of these materials, and also with the growth of bacterium *Escherichia coli*. This bacterium was selected because it represents the most common commensal bacterium physiologically present in the human intestinal tract. However, it can often act as a pathogen. Together with other gram-negative bacteria, it is a predominant microbial agent causing infections of the urinary tract. It can also contaminate vascular and urinary catheters, and form biofilms on various body implants and tissue replacements [18-21].

## 2. Experimental

Preparation and characterization of nanocomposite Ag/hydrocarbon plasma polymer films. The films were deposited on microscopic glass slides (Marienfeld, Germany, 76 x 26 x 1 mm), using an unbalanced planar magnetron with an Ag target (78 mm in diameter) operated in the dc mode in a working gas mixture of n-

hexane and argon (pressure 2 Pa, deposition time 10 min, magnetron current 0.1 A) [22]. The concentration of silver was controlled by the ratio of n-hexane and argon in the working gas mixture. The elemental concentration and its depth profiles were investigated using Rutherford Back-Scattering Spectrometry/Elastic Recoil Detection Analysis (RBS/ERDA). In addition, the concentration of silver was estimated from the sheet resistance  $R_{\square}$ . This value can serve as a parameter for determining which of the metallic

(conductive) and plasma polymer (dielectric) constituents are dominant in the composite. The material morphology and silver distribution were evaluated by Transmission Electron Microscopy (TEM; microscope Jeol FX 2000). The wettability of the composite films was estimated from the contact angle of a sessile water drop released from a syringe on to the samples (3 measurements for each experimental group).

Table 1. Physicochemical properties of composite Ag/hydrocarbon plasma polymer films.

Surface Square Resistivity, $R_{\square}$	Flow Rate Ratio n-hexane /Argon, %	Working Gas Flow, [sccm]	Average Cluster Diameter, nm	Elemental Composition, at.% *		
				Ag	C	H
1 M $\Omega$	13	7.4	20	34	38	28
6 M $\Omega$	22	7.3	15	39	33	28
20 M $\Omega$	27	7.1	10	30	38	32
900 M $\Omega$	31	7.7	-	13	69	18
4 G $\Omega$	38	6.9	7	10	59	31
5x10 <sup>3</sup> G $\Omega$	50	5.6	4	3	81	16

• Calculated from the data obtained by RBS/ERDA.

Cultures of vascular endothelial cells on nanocomposite Ag/hydrocarbon plasma polymer films. The samples were cut into square pieces of 8 x 8 mm, sterilized by ultraviolet light irradiation for 60 minutes on each side, inserted into 24-well multidishes (NUNC, Denmark, diameter 15 mm) and seeded with bovine pulmonary artery endothelial cells (line CPAE, ATCC CCL 209, Rockville, MA, USA) at an initial density of about 11,000 or 17,000 cells per cm<sup>2</sup> (i.e., 20 000 or 30 000 per well). The cells were cultured in 1.5 ml of Minimum Essential Eagle Medium supplemented with 2 mM L-glutamin, Earle's BSS with 1.5 g/L sodium bicarbonate, 0.1 mM non-essential amino acids, 1.0 mM sodium pyruvate (all chemicals from Sigma), 20% of foetal bovine serum (FBS; Sebak GmbH, Aidenbach, Germany) and 40  $\mu$ g/ml gentamycin (LEK, Ljubljana, Slovenia) at 37°C in a humidified air atmosphere with 5 % CO<sub>2</sub>. On days 1, 3 or 7 after seeding, the cells were fixed with 10% neutral formol, stained with hematoxylin and eosin and counted on microphotographs taken in 10 randomly chosen fields (size 0.1377 mm<sup>2</sup>) homogeneously distributed on each sample using a phase-contrast microscope (Olympus IX 50, Japan, obj. 20x) equipped with a digital DP70 camera. The size of cell spreading area, i.e., the cell-material contact area, was measured using Atlas software (Tescan Ltd., Brno, Czech Republic). Vinculin, a protein of focal adhesion plaques, beta-actin, an important component of cytoplasmatic cytoskeleton, and von Willebrand factor, a marker of endothelial cell maturation [23], were visualized by immunofluorescence

staining. The cells were fixed by methanol (at -20°C for 10 min), pretreated with 1% bovine serum albumin in phosphate-buffered saline (PBS) containing 0.1% Triton-X100 (Sigma, St. Louis, MO, U.S.A.) for 30 min, and then incubated with primary mouse monoclonal antibodies against vinculin (Sigma, Cat. No. V 9131, dilution 1:100) or beta-actin (Sigma, Cat. No. A 5441, dilution 1:200), or rabbit polyclonal antibody against von Willebrand factor (Sigma, Cat. No. F 3520, dilution 1:200). The primary antibodies were diluted in PBS and applied overnight at 4°C. As a secondary antibody after staining with mouse monoclonal antibodies, we used goat anti-mouse IgG, Fab specific, conjugated with fluorescein isothiocyanate (FITC; Sigma, Cat. No. F-8771, dilution 1:200). After staining with the rabbit polyclonal antibody, we used FITC-conjugated goat anti-rabbit IgG, whole molecule (Sigma, Cat. No. F-1262, dilution 1:40). The secondary antibodies were diluted in PBS and applied for 60 min at room temperature. The cells were then mounted in Gel/MountTM (Biomedica Corp., CA, U.S.A.) and evaluated using an Olympus IX 50 epifluorescence microscope.

For each experimental group, four independent samples were used. Microscopic glass slides coated with hydrocarbon plasma polymer films and uncoated glass slides served as control samples.

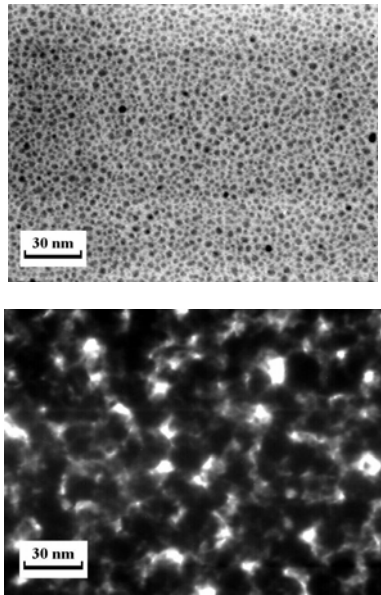


Fig. 1. Transmission electron micrographs of Ag/hydrocarbon plasma polymer composite films. A.  $R_s = 5 \times 10^3 \text{ G}\Omega$ , 3 at.% of Ag; B.  $R_s = 1 \text{ M}\Omega$ , 34 at.% of Ag.

**Cultures of *E. coli* in the presence of nanocomposite Ag/hydrocarbon plasma polymer films.** The samples in 24-well multidishes (see above) were inoculated with bacterium *Escherichia coli* C122 (prototroph, British Culture Collection, strain No. 122). Each well contained on an average 1 500 bacterial cells and 2 ml of LB medium (bacto-tryptone 10 g/l, bacto-yeast extract 5 g/l, NaCl 10 g/l in H<sub>2</sub>O). Static cultures were incubated at 37 °C for 1 to 6 h. For each experimental group, three parallel samples were used. At 1-hour intervals, the cultures were mixed with a sterile pipette in order to obtain a homogeneous bacterial suspension and immediately 5 µl aliquots were taken out from each sample. The aliquots were diluted in 20 µl of Stop buffer (1% formaldehyde, 0.25% glutaraldehyde in Sörensen phosphate buffer, pH 7.2) in order to terminate bacterial growth. Finally, the amounts of bacterial cells were counted in a Bürker counting chamber.

### 3. Results

The concentration of silver in the films increased proportionally to the amount of Ar in the working gas mixture, ranging from 0% to 39%, as estimated by RBS/ERDA (Tab. 1). Transmission electron microscopy revealed that Ag formed dark nanoclusters randomly dispersed in a lighter plasma polymer matrix, and the size of these clusters increased with silver concentration (Fig. 1, see also [22]). Static water drop contact angle measurements showed an increase in wettability on the films with relatively high sheet resistance (more than 10 MΩ), and it correlated with an evident slump in silver concentration in the films (Fig. 2).

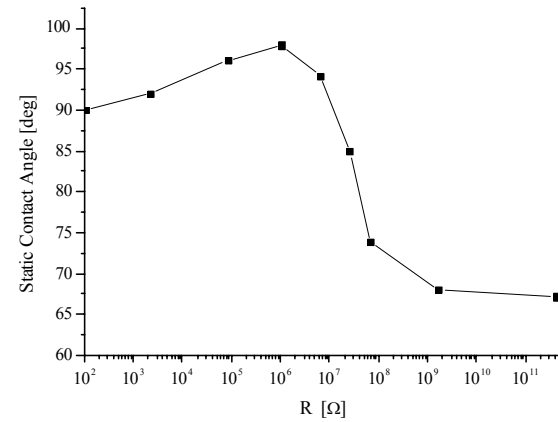


Fig. 2. Sessile water drop contact angle measured on Ag/hydrocarbon plasma polymer films versus sheet resistance ( $R_s$ ), representing the concentration of Ag.

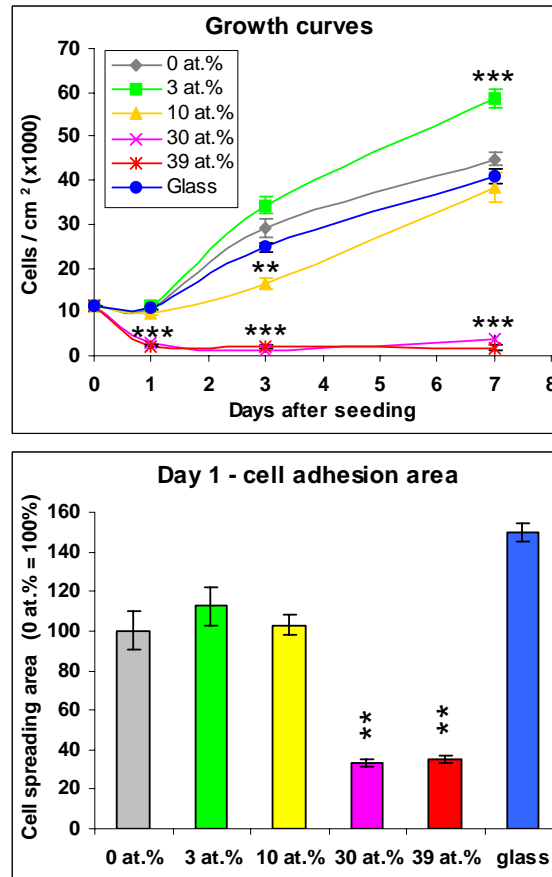


Fig. 3. Growth curves (A) and size of the cell spreading area (B) of vascular endothelial cells of the line CPAE in cultures on hydrocarbon plasma polymer films containing 0 to 39 at.% of Ag. Mean  $\pm$  S.E.M. (Standard Error of Mean). Student's *t*-test for unpaired data, statistical significance: \*\* $p \leq 0.01$  and \*\*\* $p \leq 0.001$  compared to the values on pure hydrocarbon polymer films.

The CPAE cells on day 1 after seeding adhered to the films with 3 at.% of Ag in similar numbers ( $6620 \pm 300$  cells/cm<sup>2</sup>) and by a similar cell spreading area ( $3400 \pm 390$   $\mu\text{m}^2$ ) as on the control pure hydrocarbon plasma polymer films (number  $5940 \pm 230$  cells/cm<sup>2</sup>, area  $2820 \pm 490$   $\mu\text{m}^2$ ) or glass slides (number  $5840 \pm 240$  cells/cm<sup>2</sup>, area  $3740 \pm 320$   $\mu\text{m}^2$ , Fig. 3 A, B). Immunofluorescence staining of the cells on films with 3 at.% of Ag showed numerous and bright dot-like vinculin-containing focal adhesion plaques, which were even more apparent than on the control pure hydrocarbon plasma polymer films (Fig. 4 A, B). Also beta-actin cables and Weibel-Palade bodies containing von Willebrand factor, a marker of endothelial cell maturation, were well developed in the CPAE cells on films with 3 at.% of Ag (Fig. 4 C, D). On day 7 after seeding, the cells

on these films developed confluent layers of cobblestone-like pattern, typical for mature endothelium (Fig. 4 E), and reached a significantly higher final cell population density than on pure hydrocarbon films (Fig. 3 A). In contrast, the cells on films with 30 and 39 at.% of silver adhered at very low initial numbers, did not spread and usually died before day 7 of cultivation (Figs. 3 and 4 F). All silver-containing films, including those with the lowest Ag concentration, attenuated the growth of *E. coli*. The number of bacteria in wells with glass coated with Ag-containing films did not change significantly during 6 hours after inoculation, whereas the values on pure polystyrene dishes or on pure hydrocarbon polymer films increased by at least one order of magnitude after 4-hour cultivation (Fig. 5).

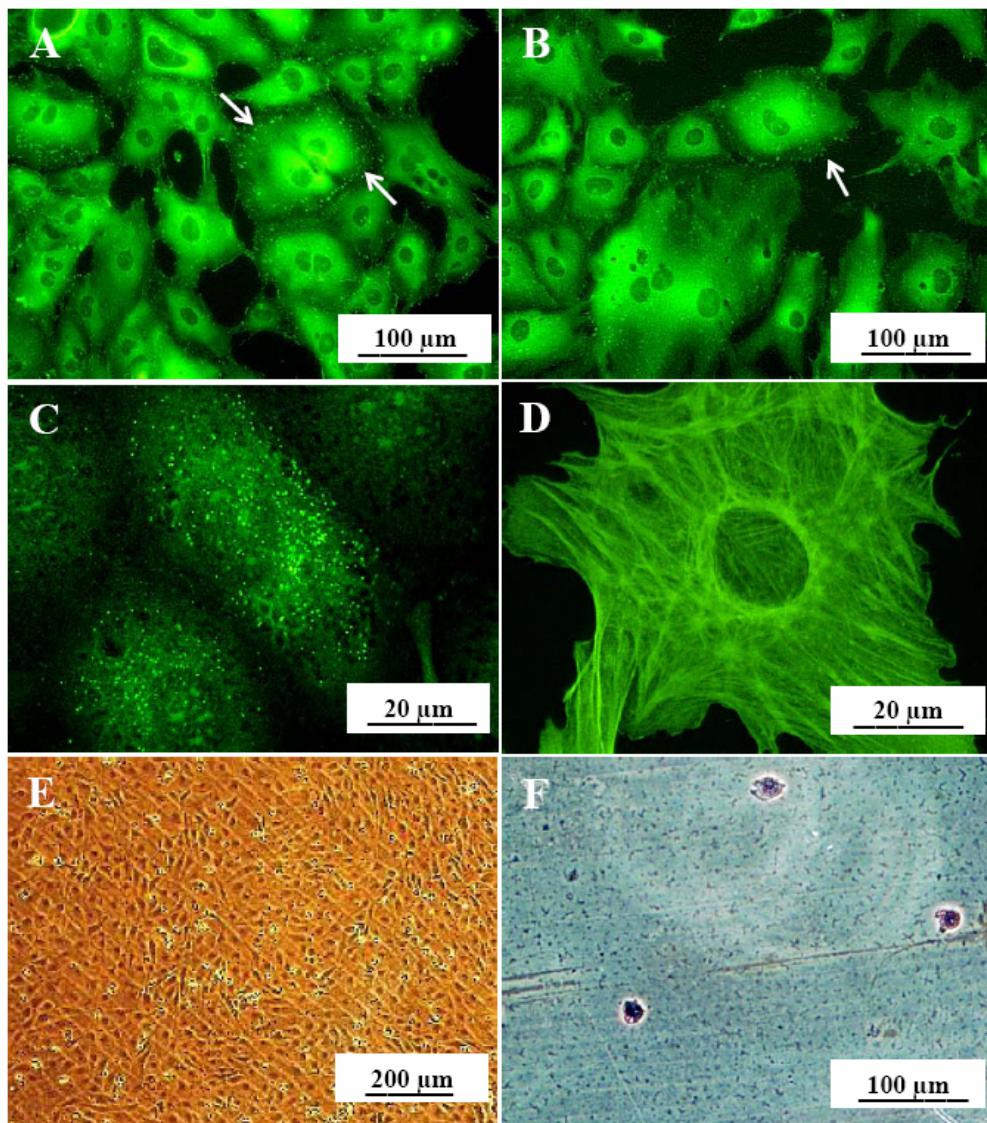


Fig. 4. Immunofluorescence staining of vinculin (A, B), a protein of focal adhesion plaques (arrows), beta-actin, a protein of cytoplasmic cytoskeleton (C) and von Willebrand factor, a marker of endothelial cell maturation (D) in CPAE cells on day 3 after seeding on films with 3 at.% of Ag (A, C, D) or 0 at.% of Ag (B). Morphology of endothelial cells on day 7 after seeding on films with 3 at.% of Ag (E) and 39 at.% of Ag (F). Microscope Olympus IX 50, camera DP 70. Obj. 20x and bar 100  $\mu\text{m}$  (A, B, F), obj. 100x and bar 20  $\mu\text{m}$  (C, D), obj. 4x and bar 200  $\mu\text{m}$  (E).

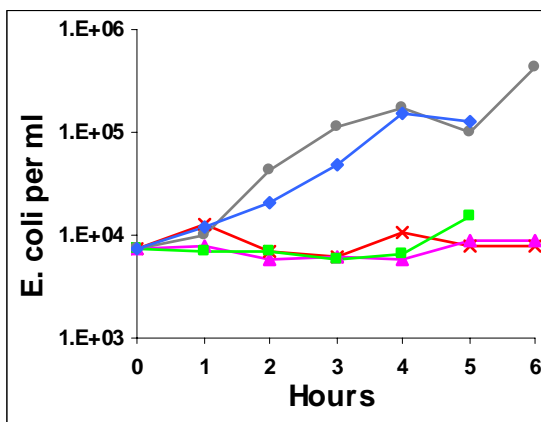


Fig. 5. Growth of *E. coli* on polystyrene dishes (blue), hydrocarbon plasma polymer films without Ag (gray), with 3 at.% Ag (green), with 30 at.% Ag (pink) or with 40 at.% Ag (red).

#### 4. Discussion

The nanocomposite Ag/hydrocarbon plasma polymer films with 3 at.% of silver supported adhesion, growth and maturation of vascular endothelial cells to an extent comparable with or even higher than on the control surfaces, represented by pure hydrocarbon plasma polymer films or glass. Moreover, the cells on the surfaces with 3 at.% of Ag showed markedly developed vinculin-containing focal adhesion plaques. Similar results were obtained in a rat mast cell line RBL-2H3 exposed to subtoxic concentrations of  $\text{Ag}^+$  ranging from 10 to 100  $\mu\text{M}$ , which induced degranulation and the release of histamine and leukotrienes via activation of focal adhesion kinase [24]. Adhesion of vascular endothelial cells was also enhanced on polystyrene implanted with  $\text{Ag}^+$  ions [25]. However, this effect seems to be due to the degradation of the polymer by the ion bombardment followed by the polymer oxidation and the increase in its wettability, rather than due to a direct action on  $\text{Ag}^+$  ions entrapped in the polymer structure. Similarly, also in the present study, the improved cell adhesion on films with the lowest silver concentration may be due by their appropriate surface wettability. It is supposed that moderate wettability of the biomaterial surface enable the adsorption of cell adhesion-mediating extracellular matrix (ECM) molecules in the optimum amount, spectrum, spatial conformation and accessibility for cell adhesion receptors, mainly integrins [23, 26]. Another factor contributing to the good cell adhesion on films with 3 at.% of Ag could be their surface nanoroughness. Similarly as moderately hydrophilic surfaces, also nanostructured surfaces promote the adsorption of ECM molecules in an appropriate spectrum and spatial conformation [27]. In addition, the increasing nanoscale surface roughness of the adhesion substrate has been shown to have a positive influence on cell functioning. Human osteoblast-like cells

of the line SAOS-2 in cultures on nanocrystalline diamond layers showed increasing activity of cellular dehydrogenases with the increasing surface roughness (the root mean square roughness,  $r_{\text{ms}}$ , was in the range from 11 nm to 39 nm) [28]. The diameter of silver nanoclusters in our films also increased from 4 nm to 20 nm, but at higher silver concentration, the supportive effects of the substrate nanostructure on its colonization with CPAE cells was disabled by the cytotoxicity of silver.

After binding the adsorbed ECM molecules, the integrins are recruited into focal adhesion plaques, in which these receptors communicate with a broad spectrum of specific structural and signalling molecules, including vinculin or focal adhesion kinase. Focal adhesion sites also serve as anchors for actin cytoskeleton and play an important role in regulating the cell behavior, such as switching between cell proliferation and differentiation, survival or apoptosis [23, 26]. Thus, the better assembly of focal adhesion plaques in CPAE cells on hydrocarbon plasma polymer films with 3 at.% of Ag may also explain the presence of well developed beta-actin cables and Weibel Palade bodies containing von Willebrand factor in these cells. Interestingly, at the same time, the films with 3 at.% of Ag attenuated the growth of bacteria *E. coli*. However, this promising result should be further investigated, particularly using culture media of the same chemical composition for both CPAE cells and *E. coli*. It has been reported that the serum supplement of the culture media used in our study for cultivating CPAE cells has protective effects against the cytotoxic action of silver [29, 30].

On films with higher Ag concentrations (30 to 39 at.%), the CPAE cells were not able to grow and survive. This finding can be explained by the inhibitory action of silver on DNA synthesis and by other cytotoxic effects of this element, such as damage and loss of cellular proteins, mitochondrial dysfunction, inhibition of adenosine triphosphate synthesis and increased generation of oxygen radicals [29, 30]. The growth of *E. coli* in presence of silver was also attenuated. Silver ions can bind bacterial DNA, inactivate bacterial proteins, inhibit a number of important transport processes of bacterial cells and interact with cellular oxidation processes as well as the respiratory chain. The  $\text{Ag}^+$  induced antibacterial killing rate is directly proportional to  $\text{Ag}^+$  concentrations, typically acting at multiple targets [18-21].

#### 5. Conclusions

Hydrocarbon plasma polymer films with 3 at.% of Ag proved to be good substrates for cultivation of vascular endothelial cells. At the same time, they showed antimicrobial activity. Thus, these films could be used for coating long-term body implants, such as intravascular stents, heart valves, the inner surface of vascular prostheses or bone implants. Films with 30 and 39 at.% of Ag were highly cytotoxic, and could be suitable for

antimicrobial coating of intravascular and urinary catheters for short-term insertion.

### Acknowledgements

This study was supported by the Acad. Sci. CR (Grant No. KAN101120701). We also thank Mrs. Ivana Zajanova (Inst. Physiol., Acad. Sci. CR) for her excellent technical assistance. Mr. Robin Healey (Czech Technical University, Prague) is gratefully acknowledged for his language revision of the manuscript.

### References

- [1] R. d'Agostino, F. Cramarossa, F. Fracassi, F. Illuzzi, *Plasma Deposition, Treatment and Etching of Polymers*, Academic Press (1990).
- [2] H. Biederman, *Plasma Polymer Films*, Imperial College Press, London (2004).
- [3] S. Affatato, M. Frigo, A. Toni, *J. Biomed. Mater. Res.* **53**, 221 (2000).
- [4] S. Kihara, K. Yamazaki, K.N. Litwak, M.V. Kameneva, H. Ushiyama, T. Tokuno, D.C. Borzelleca, M. Umezawa, J. Tomioka, O. Tagusari, T. Akimoto, H. Koyanagi, H. Kurosawa, R.L. Kormos, B.P. Griffith, *Artif. Org.* **27**, 188 (2003).
- [5] M. Ball, A. O'Brien, F. Dolan, G. Abbas, J.A. McLaughlin, *J. Biomed. Mater. Res.* **70A**, 380 (2004).
- [6] S.C. Kwok, P. Yang, J. Wang, X. Liu, P.K. Chu, *J. Biomed. Mater. Res.* **70A**, 107 (2004).
- [7] M. Ip, S.L. Lui, V.K. Poon, I. Lung, A. Burd, *J. Med. Microbiol.* **55**(Pt 1), 59 (2006).
- [8] K. Davenport, F.X. Keeley, *J. Hosp. Infect.* **60**, 298 (2005).
- [9] R.Y. Hachem, K.C. Wright, A. Zermeno, G.P. Bodey, I.I. Raad, *Biomaterials* **24**, 3619 (2003).
- [10] T. Ueberueck, R. Zippel, J. Tautenhahn, I. Gastinger, H. Lippert, T. Wahlers, *J. Biomed. Mater. Res. B Appl. Biomater.* **74**, 601 (2005).
- [11] J. Auer, R. Berent, C.K. Ng, C. Punzengruber, H. Mayr, E. Lassnig, C. Schwarz, R. Puschmann, P. Hartl, B. Eber, *J. Heart Valve Dis.* **10**, 717 (2004).
- [12] M. Bosetti, A. Masse, E. Tobin, M. Cannas, *Biomaterials* **23**, 887 (2002).
- [13] M. Bellantone, H.D. Williams, L.L. Hench, *Antimicrob. Agents Chemother.* **46**, 1940 (2002).
- [14] V. Alt, T. Bechert, P. Steinrucke, M. Wagener, P. Seidel, E. Dingeldein, E. Domann, R. Schnettler, *Biomaterials* **25**, 4383 (2004).
- [15] J. J. Blaker, S.N. Nazhat, A.R. Boccaccini, *Biomaterials* **25**, 1391 (2004).
- [16] N. Shanmugasundaram, J. Sundaraseelan, S. Uma, D. Selvaraj, M. Babu, *J. Biomed. Mater. Res. B Appl. Biomater.* **77**, 378 (2006)
- [17] Y.S. Choi, S.R. Hong, Y.M. Lee, K.W. Song, M.H. Park, Y.S. Nam, *J. Biomed. Mater. Res.* **48**, 631 (1999).
- [18] K. Modak, C. Fox, *Biochem. Pharm.* **22**, 2392 (1973)
- [19] J. M. Schierholz, J. Beuth, G. Pulverer, D.P. Konig, *Antimicrob. Agents Ch.* **43**, 2819 (1999)
- [20] H.-J. Jeon, S.-C. Yi, S.-G. Oh, *Biomaterials* **24**, 4921 (2003)
- [21] Z. Shi, K.G. Neoh, S.P. Zhong, L.Y. Yung, E.T. Kang, W. Wang, *J. Biomed. Mater. Res. A* **76**, 826 (2006)
- [22] H. Boldyryeva, P. Hlidek, H. Biederman, D. Slavinska, A. Choukourov, *Thin Solid Films* **442**, 86 (2003).
- [23] L. Bacakova, V. Mares, V. Lisa, V. Svorcik, *Biomaterials* **21**, 1173 (2000)
- [24] Y. Suzuki, T. Yoshimaru, K. Yamashita, T. Matsui, M. Yamaki, K. Shimizu, *Biochem. Biophys. Res. Commun.* **283**, 707 (2001)
- [25] H. Sato, H. Tsuji, S. Ikeda, N. Ikemoto, J. Isihikawa, S. Nishimoto, *J. Biomed. Mater. Res.* **44**, 22 (1999)
- [26] L. Bacakova, E. Filova, F. Rypacek, V. Svorcik, V. Stary, *Physiol. Res.* **53**, 35 (2004)
- [27] T.J. Webster, C. Ergun, R.H. Doremus, R.W. Siegel, R. Bizio, *J. Biomed. Mater. Res.* **51**, 475 (2000).
- [28] M. Kalbacova, M. Kalbac, L. Dunsch, A. Kromka, M. Vanecek, B. Rezek, U. Hempel, S. Kmoch, *Phys. Stat. Sol. (b)*, 1–4 (2007)
- [29] E. Hidalgo, R. Bartolome, C. Barroso, A. Moreno, C. Dominguez, *Skin Pharmacol. Appl. Skin Physiol.* **11**, 140 (1998)
- [30] T. Sun, S. Jackson, J.W. Haycock, S. MacNeil, J. Biotechnol. **10**, 372 (2006)

\*Corresponding author: lucy@biomed.cas.cz